

Hollow carbon spheres as an efficient dopant for enhancing critical current density of MgB₂ based tapes

Zhaoshun Gao¹, Yanwei Ma^{1,*}, Xianping Zhang¹, Dongliang Wang¹, Junhong Wang¹, K. Watanabe², Boyang Liu³

¹ Key Laboratory of Applied Superconductivity, Institute of Electrical Engineering, Chinese Academy of Sciences, P. O. Box 2703, Beijing 100080, China

² High Field Laboratory for Superconducting Materials, Institute for Materials Research, Tohoku University, Sendai 980-8577, Japan

³ Institute for Advanced Ceramics, Harbin Institute of Technology, Harbin 150001, China

Abstract:

A significant enhancement of J_c and H_{irr} in MgB₂ tapes has been achieved by the in situ powder-in-tube method utilizing hollow carbon spheres (HCS) as dopants. At 4.2 K, the transport J_c for the 850°C sintered samples reached 3.1×10^4 , and 1.4×10^4 A/cm² at 10 and 12 T, respectively, and were better than those of optimal nano-SiC doped tapes. Furthermore, the H_{irr} for doped sample was raised up to 16.8 T at 10 K due to the carbon substitution effect. The results demonstrate that HCS is one of the most promising dopants besides nano-carbon and SiC for the enhancement of current capacity for MgB₂ in high fields.

* Author to whom correspondence should be addressed; E-mail: ywma@mail.iee.ac.cn

1. Introduction

Superconducting MgB₂ tape has been regarded as a promising candidate for practical applications such as MRI magnet at around 20 K due to its high transition temperature (T_c), low material costs and weak-link free grain coupling [1]. The critical current density (J_c) of MgB₂ tapes can be easily exceed the level 10^4 A/cm² at 4.2 K and 10 T through chemical doping with carbon containing materials, such as SiC [2-4], C [5,6], B₄C [7], carbon nanotube [8], carbohydrate or hydrocarbon [9-12]. The carbon can be incorporated into the MgB₂ crystal lattice, and thus J_c and H_{c2} are significantly enhanced due to the enhancement of charge carrier scattering in the two-band MgB₂ [13,14]. It should be pointed out that the improvement of superconducting properties is sensitive to morphology of the particles and the synthesis conditions. Doping with these carbon-based materials gives rise to some concerns such as agglomeration of the particles, poor reactivity, very long milling time or gas release problems.

In order to overcome these problems, we proposed to use hollow carbon spheres (HCS) as the dopant. There are many advantages of HCS doping: First, although the diameters of HCS vary from 1 μ m to 8 μ m, the nano-scale thickness means that they can be easily broken into nano flakes by ball milling in short time. Second, the HCS have turbostratic graphite structure and very high specific surface area, hence, the carbon of HCS can be reacted with Mg and B more efficiently than other form carbon. Third, the disordered graphite sheet in HCS is somewhat similar to the arrangement of B atoms in MgB₂, it may easily cause the distortion of honeycomb B. In addition, HCS with a turbostratic graphite structure enable to reduce the friction between the core and the tube walls during deformation process. It is favor for the extent of deformation as well as the core homogeneity of long PIT tapes. In this letter, we have synthesized HCS doped MgB₂ tapes and succeeded in significantly improving the transport J_c - H properties of MgB₂ in high magnetic fields up to 14 T.

2. Experimental details

The MgB₂ composite tapes with HCS doping were prepared by the in situ PIT method. Mg powder (325 mesh, 99.8%), B powder (amorphous, 99.99%) were mixed

in a fixed of 1:2 with 1 wt.% HCS powder as additions for the fabrication of tapes. As indicated in Fig.1, the HCS with turbostratic graphite structure and several micrometers in diameter were used in this study. The details of fabricating process and properties for HCS are described elsewhere [15]. The mixtures were milled using a ball mill with agate milling tools for 1 h under air atmosphere. For HCS doped samples, before milling, about 1 ml acetone was dropped to the powder in order to achieve more homogeneity. The packing of the mixed powder into Fe tubes were carried out under a high-purity argon gas atmosphere by using a glove box in order to avoid oxidation and spontaneous combustion of the powders. For the pure samples, the packing of powder were carried out in air. After packing, the tube was rotary swaged and then drawn to wires of 1.75 mm in diameter. The wires were subsequently rolled to tapes. The final size of the tapes was about 3.8 mm in width and about 0.5 mm in thickness. These tapes were heated at 700~850 °C for 1 h, and then followed by a furnace cooling to room temperature. The high purity argon gas was allowed to flow into the furnace during the heat-treatment process to reduce the oxidation of the samples.

The phase identification and crystal structure investigation were carried out using x-ray diffraction (XRD). Microstructure was studied using a transmission electron microscopy (TEM). DC magnetization measurements were performed with a superconducting quantum interference device (SQUID) magnetometer. Resistivity curves were measured using a current of 100 mA in the high field magnet with Fe sheath, the 10% points on the resistive transition curves were used to define the H_{irr} . The transport current I_c at 4.2 K and its magnetic field dependence were evaluated at the High Field Laboratory for Superconducting Materials (HFLSM) at Sendai, by a standard four-probe resistive method, with a criterion of $1 \mu\text{V cm}^{-1}$, a magnetic field up to 14 T was applied parallel to the tape surface. For each set of doping tapes, the I_c measurement was performed for several samples to check the reproducibility.

3. Results and discussion

Figure 2 shows the results of x-ray diffraction measurements for pure and doped samples. As can be seen, all samples consisted of a main phase, MgB_2 , but some MgO

impurity phase was also detected. Table I provides an overview of the properties for pure and doped MgB₂ samples. As shown in table I, the *a* lattice parameters of all doped samples showed a noticeable decrease compared with the pure sample, while lattice parameter *c* kept almost unchanged. The shrinkage of *a* is attributed to the substitution of C for B [5, 16], as the C atom is smaller than the B atom. Furthermore, doping was also confirmed by analysis of full width at half maximum (FWHM) values as shown in Fig 3. The FWHM of the (002) and (110) peaks for the doped tapes are apparently larger than those of the corresponding peaks for the un-doped one. Broadening in peaks is a strong indication of grain size refinement and lattice distortion, the former can be observed from TEM images of HCS doped MgB₂ (Fig. 5). It's worth to note that the influence of doping on (110) peak are apparently larger than (002) peak. It might due to the disordered graphite sheet in HCS is somewhat similar to the arrangement of B atoms in MgB₂, and then cause the distortion of honeycomb B. On the other hand, FWHM values decreased with increasing sintering temperature, which is attributable to the improvement in crystallinity. An improvement in crystallinity also accompanies better grain connectivity of the MgB₂, as shown in Table I. As can be seen from Table I, *T_c* increased with increasing sintering temperature. This *T_c* increase is a result of improved crystallinity as mentioned in XRD analyses.

Figure 4 shows the transport *J_c* at 4.2 K in magnetic fields up to 14 T for HCS doped tapes annealed at 700, 800 and 850 °C, respectively. As a reference, the data of the pure tapes which were sintered at 800 °C are also included in the figure. As can be seen from Fig.4, all doped samples show a drastic enhancement of *J_c* compared with pure MgB₂ tapes. The doped tapes heated at 850 °C reveal the highest *J_c* compared to all other samples in our experiment: At 4.2 K and in a field of 12 T, the transport *J_c* reached 1.42×10^4 A/cm², more than 18-fold improvement compared to the pure samples, which have a *J_c* value about 7.7×10^2 A/cm². Also, *J_c* kept 3.1×10^4 and 6.0×10^3 A/cm² at 10 and 14 T, respectively. These *J_c* values of the tapes investigated in this work were better than those of optimal nano-SiC doped tapes [17], and highlight the importance of HCS doping for enhancing the *J_c* of MgB₂

superconductors.

In Table I the irreversibility field at 10 K, obtained from the 10% values of their corresponding resistive transitions is presented. As we can see, the H_{irr} properties of the doped MgB_2 samples are significantly enhanced. The enhancement of H_{irr} indicates that the intrinsic properties such as band scattering of MgB_2 were increased by C substitution into B sites, resulting in higher H_{c2} and hence higher H_{irr} . As shown in FWHM results, a distortion of the honeycomb B sheet caused by C substitutional effect is believed to increase the intraband scattering, and thus enhance H_{c2} and H_{irr} . As shown in Table 1, electrical resistivity (ρ) values for pure and HCS doped MgB_2 samples at 40 K were 27.4 and 160~210 $\mu\Omega$ cm respectively. The higher ρ values for the doped MgB_2 samples indicate that stronger impurity scattering is introduced by the C substitution into B sites.

Figure 5 shows the typical TEM images for HCS doped tapes. The TEM results reveal that there are a number of impurity phases in the form of nanometer-size inclusions (5–20 nm in size) inside grains in the HCS doped samples [see Figs. 5(a) 5(b)]. As the coherence length of MgB_2 is about 6–7 nm [18], these 5–20 nm-sized inclusions, with a high density, are ideal flux pinning centres and are responsible for the better J_c performance in doped samples. The selected area diffraction (SAD) pattern, shown in the corner of Fig.5a, consists of very well defined ring patterns, suggesting a very fine grain size. The high-resolution TEM images also show very fine MgB_2 grains with size about 10 nm. Obviously, the fine grain size would create many grain boundaries that may act as effective pinning centres and raise H_{c2} by scattering electrons [19]. The reduction in grain size is probably explained by the inhibition of grain growth by finely dispersed second phases introduced by the doping and milling process [20].

It is well confirmed now that C substitution into B sites results in an enhancement in J_c -H and H_{irr} [2–12]. Due to the special structure of HCS, they can be broken into nano flakes by ball milling. These carbon nano flakes would be easily incorporated into the crystal lattice of MgB_2 , then substitute into B sites via the reaction. The large distortion of the crystal lattice caused by carbon substitution for B leads to enhanced

electron scattering and enhancement of H_{c2} and H_{irr} . The finely dispersed second particles observed by TEM examinations have two functions: first, they can act as nucleation sites to refine the MgB_2 grains and hence raise the pinning force and H_{c2} . Second, these particles can be included within the grains as nano-inclusions, which can enhance the flux pinning directly. Therefore, C substitution-induced H_{irr} enhancement as well as the strong flux pinning centers induced by grain boundaries and nanosized inclusions are responsible for the superior J_c - H performance of the doped samples.

4. Conclusions

In summary, we have demonstrated that both the transport J_c and H_{irr} of MgB_2 tapes are all significantly enhanced by HCS. We believe that this is due to a high level of carbon substitution in the MgB_2 lattice. C substitution for B sites increases the intraband scattering, and thus enhances H_{c2} and H_{irr} . On the other hand, High density grain boundaries and nanosized inclusions introduced by HCS doping significantly enhance the pinning force and hence drastically improve J_c - H performance.

Acknowledgments

The authors thank Haihu Wen, Huang Yang, Liye Xiao and Liangzhen Lin for their help and useful discussion. This work is partially supported by the Beijing Municipal Science and Technology Commission under Grant No. Z07000300700703, National ‘973’ Program (Grant No. 2006CB601004) and National ‘863’ Project (Grant No. 2006AA03Z203).

References

- [1] Y. Iwasa, D. C. Larbalestier, M. Okada, R. Penco, M. D. Sumption, and X. Xi, IEEE Trans. Appl. Supercond. **16**, 1457 (2006).
- [2] S. X. Dou, S. Soltanian, J. Horvat, X. L. Wang, S. H. Zhou, M. Ionescu, H. K. Liu, P. Munroe, and M. Tomsic, Appl. Phys. Lett. **81**, 3419 (2002).
- [3] H. Kumakura, H. Kitauchi, A. Matsumoto, and H. Hatakeyama, Appl. Phys. Lett. **84**, 3669 (2004).
- [4] M. D. Sumption, M. Bhatia, M. Rindfleisch, M. Tomsic, S. Soltanian, S. X. Dou, and E. W. Collings, Appl. Phys Lett. **86**, 092507 (2005).
- [5] M. Herrmann, W. Häßler, C. Rodig, W. Gruner, B. Holzapfel, and L. Schultz, Appl. Phys. Lett. **91**, 082507 (2007).
- [6] Yanwei Ma, Xianping Zhang, G. Nishijima., K. Watanabe, S. Awaji and Xuedong Bai, Appl. Phys. Lett. **88**, 072502 (2006).
- [7] P Lezza, C Senatore and R Flükiger, Supercond. Sci. Technol. **19**, 1030 (2006).
- [8] J. H. Kim, W. K. Yeoh, M. J. Qin, X. Xu, and S. X. Dou, Appl. Phys. Lett. **89**, 122510 (2006).
- [9] J. H. Kim, S. Zhou, M. S. A. Hossain, A. V. Pan, and S. X. Dou, Appl. Phys. Lett. **89** 142505 (2006)
- [10]Zhaoshun Gao, Yanwei Ma, Xianping Zhang, Dongliang Wang, Zhengguang Yu, Huan Yang Haihu Wen and E Mossang, J. Appl. Phys. **100**, 013914 (2007).
- [11]Zhaoshun Gao, Yanwei Ma, Xianping Zhang, Dongliang Wang, Huan Yang Haihu Wen and K Watanabe, Appl. Phys. Lett. **91** 162504 (2007).
- [12]H. Yamada, M. Hirakawa, H. Kumakura, and H. Kitaguchi, Supercond. Sci. Technol. **19**, 175 (2006).
- [13]A. Gurevich, Phys. Rev. B **67** 184515 (2003).
- [14]A. Gurevich *et al* Supercond. Sci. Technol. **17** 278 (2004).
- [15]Boyang Liu, Dechang Jia, Qingchang Meng and Jiancun Rao, Carbon **45** 668 (2007)
- [16]S. Lee, T. Masui, A. Yamamoto, H. Uchiyama, and S. Tajima, Physica C **397**, 7 (2003).
- [17]S. X. Dou *et al* Phys. Rev. Lett. **98** 097002 (2007)
- [18]D. K. Finnemore, J. E. Ostenson, S. L. Bud'ko, G. Lapertot, and P. C. Canfield Rev. Lett. **86** 2420 (2001)
- [19]H. Kitaguchi, A. Matsumoto, H. Kumakura, T. Doi, H. Sosiati, and S.Hata, Appl. Phys. Lett. **85**, 2842 (2004)
- [20]Ben J Senkowicz, R J Mungall, Y Zhu, Jiangyi Jiang, Paul Voyles, Eric Hellstrom and D C Larbalestier, arXiv:0712.2056

TABLE I. Some superconducting properties for pure and HCS doped samples

Sample	Lattice (Å)	T_c (K)	RRR	ρ_{40} ($\mu\Omega\text{cm}$)	J_c (4.2K, 12 T)	H_{irr} (T) at 10 K
Pure	3.083	37	1.95	30.9	7.7×10^2	12.4
700 °C	3.071	30.2	1.29	208.1	5.6×10^3	
800 °C	3.068	30.9	1.28	199.6	1.0×10^4	15.8
850 °C	3.069	31.5	1.33	168.3	1.4×10^4	16.8

Captions

- Figure 1 TEM image of HCS showing hollow structure (a), XRD pattern of the HCS (b), HRTEM image of fine structure of the shell near the surface of one HCS is shown in the corner of Fig.1a.
- Figure 2 XRD patterns of in situ processed pure and doped tapes. The peaks of MgB_2 indexed, while the peaks of MgO are marked by *.
- Figure 3 FWHM values of various diffraction peaks as a function of samples.
- Figure 4 J_c - H properties of Fe-sheathed pure and doped tapes. The data of nano-SiC doped tapes are also included in the figure for comparison [17].
- Figure 5 The TEM images for HCS doped samples sintered at 800 °C (a, c) and 850 °C (b, d).

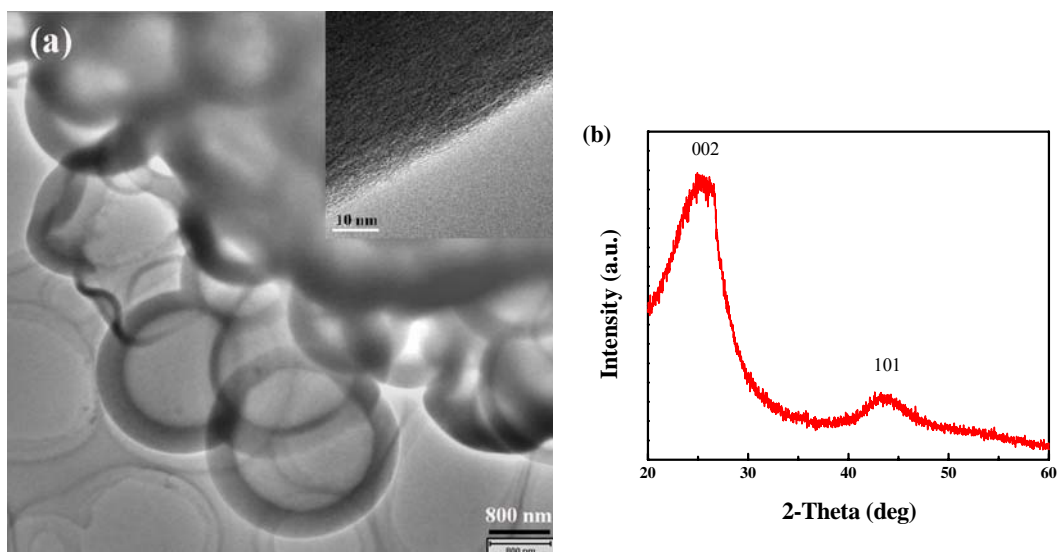


Fig.1 Gao et al.

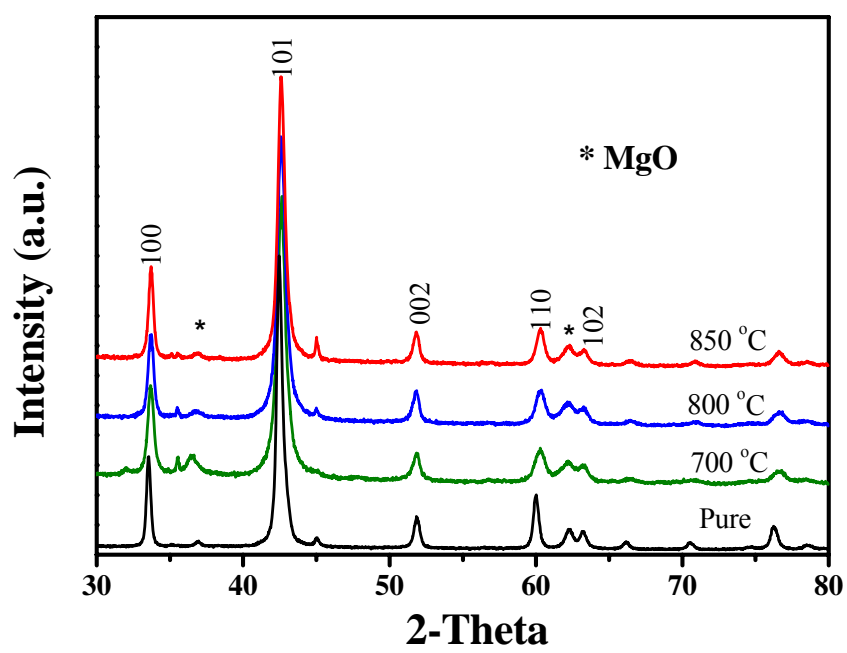


Fig.2 Gao et al.

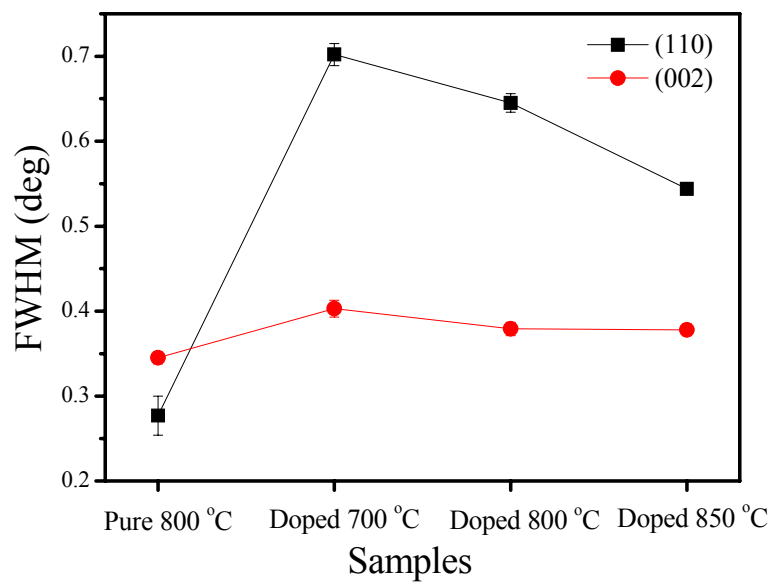


Fig.3 Gao et al.

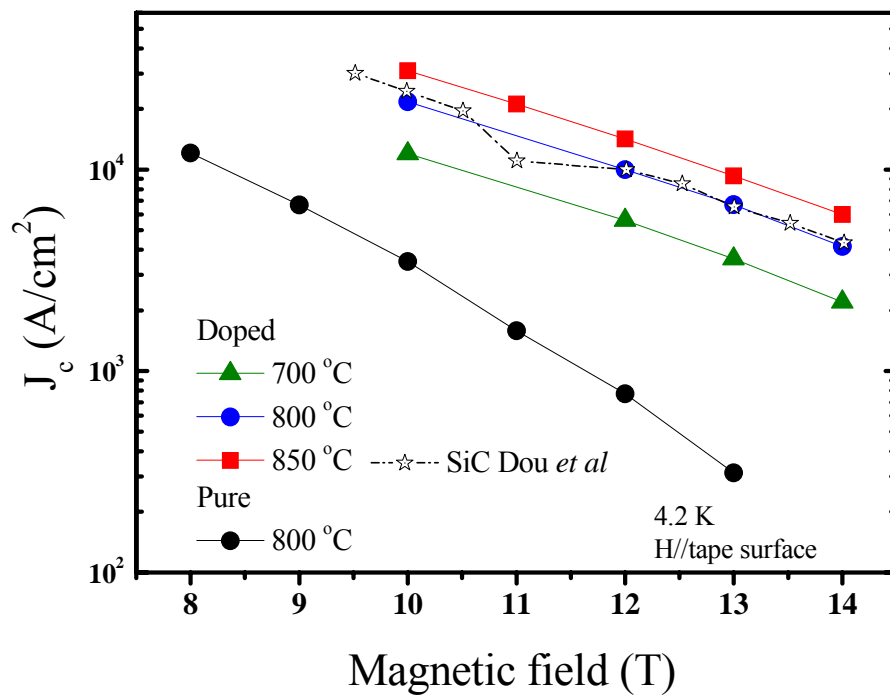


Fig.4 Gao et al.

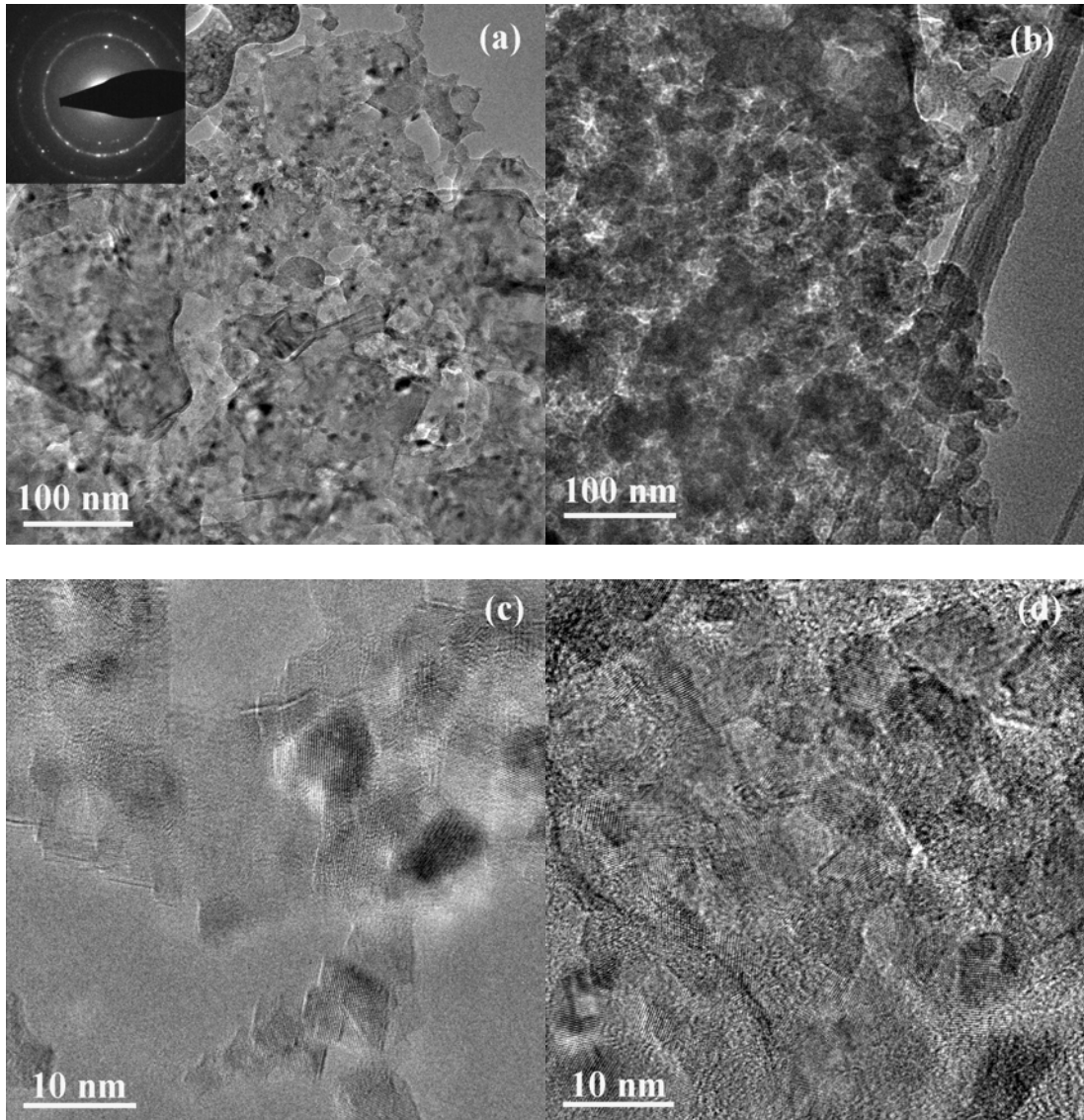


Fig.5 Gao et al.